

A Unified Framework for Spherical Matrix Factorization

Kai Liu *

Abstract

Matrix Factorization plays an important role in machine learning such as Non-negative Matrix Factorization, Principal Component Analysis, Dictionary Learning, *etc.* However, most of the studies aim to minimize the loss by measuring the Euclidean distance, though in some fields, angle distance is known to be more important and critical for analysis. In this paper, we propose a method by adding constraints on factors to unify the Euclidean and angle distance. However, due to non-convexity of the objective and constraints, the optimized solution is not easy to obtain. In this paper we propose a general framework to systematically solve it with provable convergence guarantee with various constraints.

1 Introduction

Principal Component Analysis (PCA) is widely known to be one of the most popular methods for dimension reduction. Mathematically, assume that we have a set of n sample images $\mathbf{X} = [\mathbf{x}_1, \mathbf{x}_2, \dots, \mathbf{x}_n] \in \mathbb{R}^{m \times n}$, where $\mathbf{x}_i \in \mathbb{R}^m$ and $i \in [1, n]$ denotes the i -th data (WLOG, we assume the data is centralized). The objective of PCA is to minimize the error between original data and reconstruction under new base $\mathbf{W} \in \mathbb{R}^{m \times r}$ (r denotes the reduced dimension):

$$\min_{\mathbf{W}} h = \|\mathbf{X} - \mathbf{W}\mathbf{V}\|_F^2, \quad s.t. \quad \mathbf{W}^T \mathbf{W} = \mathbf{I}, \quad (1)$$

where $\|\cdot\|_F$ denotes the Frobenius norm of a matrix. Apparently, if there is no constraint on \mathbf{V} , then by taking the derivative of h w.r.t. \mathbf{V} and set to be 0, then $\mathbf{V}^* = \mathbf{W}^T \mathbf{X}$. \mathbf{W} contains the principal directions and \mathbf{V} indicates the principal components (data projects along the principal directions). However, when it is to optimize sparse components, namely \mathbf{V} is imposed with sparsity constraint, $\mathbf{W}^T \mathbf{X}$ is no longer the optimal solution [1].

Another example is Nonnegative Matrix Factorization (NMF), which aims to find two nonnegative matrices, $\mathbf{U} \in \mathbb{R}_+^{m \times r}$ and $\mathbf{V} \in \mathbb{R}_+^{r \times n}$, whose product can best approximate an input nonnegative data matrix $\mathbf{X} \in \mathbb{R}_+^{m \times n}$, *i.e.*, $\mathbf{X} \approx \mathbf{U}\mathbf{V}$. Usually, one can interpret the columns of \mathbf{X} as data points and the rows of \mathbf{X} as observations (features). A broadly used objective to learn NMF is to minimize the following objective:

$$\min_{\mathbf{U}, \mathbf{V} \geq 0} h(\mathbf{U}, \mathbf{V}) = \frac{1}{2} \|\mathbf{X} - \mathbf{U}\mathbf{V}\|_F^2. \quad (2)$$

If we consider the r columns of \mathbf{U} the basis vectors, every column of \mathbf{V} approximates the corresponding data point in \mathbf{X} by a linear combination of these r bases vectors, where the elements of the column of \mathbf{V} specify the coefficients to compute the linear combination. NMF has been found useful in a large variety of real-world applications such as image feature extraction [2, 3], document clustering [4, 5, 6], single

*Computer Science Division, Clemson University. kail@clemson.edu

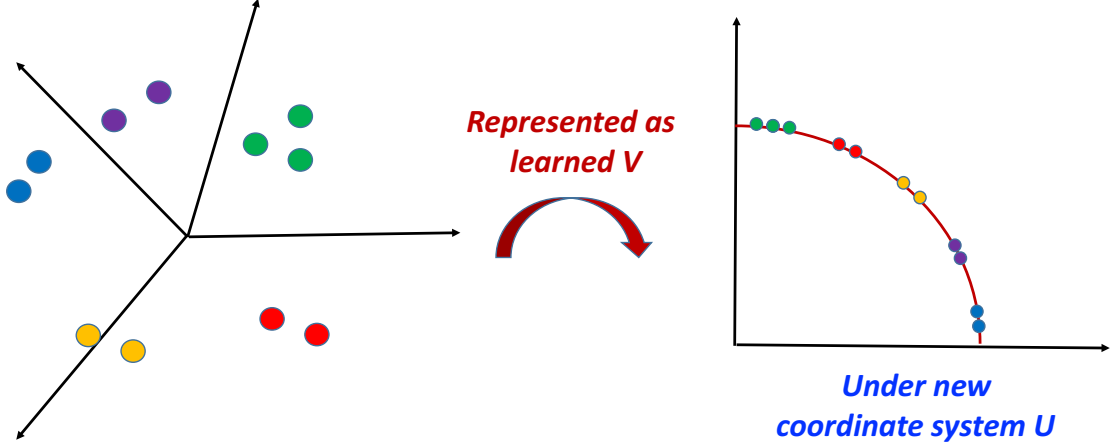


Figure 1: Data in original high dimension ($m = 4$) can be analysed (such as clustered or classified) in lower dimension ($r = 2$) space, where all data points lie in the sphere under new coordinate system. Since we have nonnegative constraint on V , they all lie in the first quadrant.

speech separation [7], music transcription [8], bioinformatics [9, 10, 11, 12], recommendation system [13], astronomy [14, 15], to name a few.

To solve the NMF objective in Eq. (2), a Multiplicative Updating Algorithm (MUA) was derived using the following updating rules [16]:

$$V_{ij} \leftarrow V_{ij} \frac{(U^T X)_{ij}}{(U^T UV)_{ij}}, \quad U_{ij} \leftarrow U_{ij} \frac{(XV^T)_{ij}}{(UVV^T)_{ij}}.$$

The convergence of this algorithm was proved using the auxiliary function method [16], whose correctness was also analysed in [17].

Following the updating algorithm listed above, many NMF-based learning methods have been proposed. For instance, to guarantee the uniqueness of U and V , orthogonal constraints were used in [18]:

$$\min_{U, V \geq 0} h(U, V) = \frac{1}{2} \|X - UV\|_F^2, \quad s.t. \quad U^T U = I. \quad (3)$$

To include the mixed signs of the data matrix, Semi-NMF objective was studied in [17]:

$$\min_{V \geq 0} h(U, V) = \frac{1}{2} \|X - UV\|_F^2. \quad (4)$$

Inspired by the examples illustrated above and more (such as Dictionary Learning, *etc.*), it is noticeable that matrix factorization plays an important role in classical machine learning. Different constraints will lead to various names, but the nature is similar: to approximate the data with linear combinations of learned basis (can be orthogonal such as in PCA and orthogonal dictionary learning).

2 Motivation and Our Contributions

In Eq. (1–4), the objectives minimize difference between original data X and approximated reconstruction data UV , which is measured by squared Euclidean distance and treat each feature equally important. However, in real world applications, there exist datasets where distance-based measurement method may yield

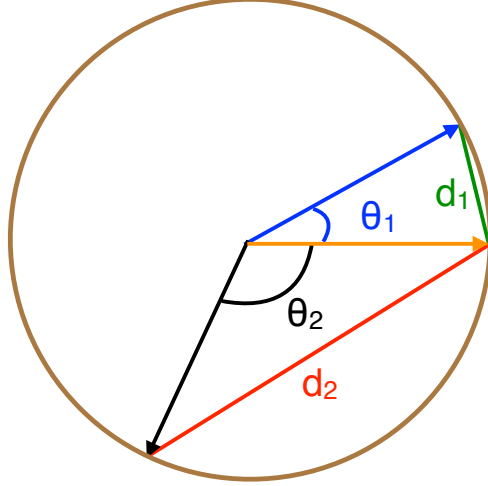


Figure 2: Larger angle distance ($\theta_2 > \theta_1$) in the sphere will have larger Euclidean distance ($d_2 > d_1$), and vice versa, which unifies the cosine similarity and Euclidean distance.

poor results [19]. In contrast, similarity-based measurements, such as angle distance, have been found wide successful applications in information retrieval [20, 21], signal processing [22], metric learning [23], and so on. Although one can calculate the similarity (cosine distance) from the vectors in \mathbf{V} , after all it is an indirect method which is usually not effective. Therefore, deriving a direct method that can straightforwardly measure angle distance from Matrix Factorization (MF) is important and urgent.

With the above motivation, in this paper we propose a general framework for **Spherical Matrix Factorization** model which unifies Euclidean and angle distance. As illustrated in Fig. 1, we assume that each data point in \mathbf{X} that reside in the original high-dimensional space (\mathbb{R}^m) can be represented as \mathbf{V} in a lower dimensional space (\mathbb{R}^r) under new coordinate system \mathbf{U} . By noticing that larger angle in the sphere in Fig. 2 also has larger Euclidean distance, we can add the normalization constraint to the component matrix \mathbf{V} to guarantee the spherical distribution of components:

$$\begin{aligned} \min_{\mathbf{U} \in \mathbb{R}^{m \times r}, \mathbf{V} \in \mathbb{R}^{r \times n}} h = \|\mathbf{X} - \mathbf{UV}\|_F^2 = \sum_{i,j} [\mathbf{X}_{ij} - (\mathbf{UV})_{ij}]^2 \\ \text{s.t. } \mathbf{U} \in \mathbb{U}, \mathbf{V} \in \mathbb{V}, \end{aligned} \quad (5)$$

where $\mathbb{U} = \mathbb{U}_1 \cup \mathbb{U}_2$, $\mathbb{V} = \mathbb{V}_1 \cup \mathbb{V}_2 \cup \mathbb{V}_3 \cup \mathbb{V}_4$ and

$$\begin{aligned} \mathbb{U}_1 &:= \{\mathbf{U} \mid \mathbf{U}^T \mathbf{U} = \mathbf{I}\}, \mathbb{U}_2 := \{\mathbf{U} \mid \mathbf{U} \geq 0\}; \\ \mathbb{V}_1 &:= \{\mathbf{V} \mid \|\mathbf{V}(:, j)\| = l, \forall j\}, \mathbb{V}_2 := \{\mathbf{V} \mid \mathbf{V} \geq 0, \|\mathbf{V}(:, j)\| = l, \forall j\}, \\ \mathbb{V}_3 &:= \{\mathbf{V} \mid \|\mathbf{V}(:, j)\| = l, \|\mathbf{V}(:, j)\|_0 \leq s, \forall j\}, \mathbb{V}_4 := \{\mathbf{V} \mid \mathbf{V} \geq 0, \|\mathbf{V}(:, j)\| = l, \|\mathbf{V}(:, j)\|_0 \leq s, \forall j\}. \end{aligned} \quad (6)$$

One can see that when $\mathbf{U} \in \mathbb{U}_2$, $\mathbf{V} \in \mathbb{V}_2$, it is Spherical Non-negative Matrix Factorization; when $\mathbf{U} \in \mathbb{U}_1$, $\mathbf{V} \in \mathbb{V}_1$, it is Spherical PCA, and so on. Suppose the component is spherically distributed (with l

representing sphere radius), then the Euclidean distance between \mathbf{v}_i and \mathbf{v}_j is:

$$\|\mathbf{v}_i - \mathbf{v}_j\|_2^2 = \|\mathbf{v}_i\|^2 + \|\mathbf{v}_j\|^2 - 2\langle \mathbf{v}_i, \mathbf{v}_j \rangle \quad (7)$$

$$\begin{aligned} &= \|\mathbf{v}_i\|^2 + \|\mathbf{v}_j\|^2 - 2 \frac{\langle \mathbf{v}_i, \mathbf{v}_j \rangle}{\|\mathbf{v}_i\| \|\mathbf{v}_j\|} \\ &= 2l^2 - 2 \cos(\theta), \theta \in [0, \pi], \end{aligned} \quad (8)$$

which illustrates that larger angle θ will yield larger Euclidean distance, and vice versa.

In the rest of this paper, we will propose a general but efficient framework to solve Eq. (5) where constraints are varied in Eq. (6). Here we summarize our contributions explicitly as follows:

- We propose a matrix factorization model that unifies Euclidean and angle distance, which can work well on various datasets.
- We systematically propose a wild framework which will make the objective monotonically decreasing while strictly satisfying constraints.
- Our algorithm not only can guarantee the monotonically decreasing property of the objective, but also can guarantee the global-sequence convergence property of \mathbf{U} and \mathbf{V} with at least sub-linear convergence rate.

3 Formulation And Algorithm

We first denote:

$$h(\mathbf{U}, \mathbf{V}) = \|\mathbf{X} - \mathbf{UV}\|_F^2, \quad s.t. \quad \mathbf{U} \in \mathbb{U}, \mathbf{V} \in \mathbb{V}. \quad (9)$$

By noting that Eq. (5) is non-convex, for which no closed solution exists, a natural idea is to use alternating minimization method to solve the optimization problem:

$$\begin{aligned} \mathbf{U}_{k+1} &= \arg \min \|\mathbf{X} - \mathbf{UV}_k\|_F^2, \quad \mathbf{U} \in \mathbb{U}, \\ \mathbf{v}_{k+1} &= \arg \min \|\mathbf{x} - \mathbf{U}_{k+1}\mathbf{v}\|_F^2, \quad \mathbf{V} \in \mathbb{V}, \end{aligned} \quad (10)$$

where \mathbf{v} denotes the column of \mathbf{V} , as the optimization problem in Eq. (5) with respect to \mathbf{V} can be decoupled into column-wise sub-problems.

For the past decade, proximal algorithm has been successfully applied to solve a wide variety of problems, such as convex optimization, non-monotone operators [24, 25] with various applications to non-convex programming. More recently, proximal alternating linearized minimization (PALM) was introduced [26] as a linearized approximation of the proximal algorithm. Considering the fact that objective function in Eq. (5) is non-convex w.r.t. \mathbf{U} and \mathbf{V} , plus the constraints on \mathbf{U} , \mathbf{V} is non-convex, we utilize PALM and optimize the solution as:

$$\mathbf{U}_{k+1} = \arg \min_{\mathbf{U} \in \mathbb{U}} \langle \mathbf{U} - \mathbf{U}_k, \nabla h_{\mathbf{U}}(\mathbf{U}_k, \mathbf{V}_k) \rangle + \frac{\mu}{2} \|\mathbf{U} - \mathbf{U}_k\|_F^2, \quad (11)$$

$$\mathbf{v}_{k+1} = \arg \min_{\mathbf{V} \in \mathbb{V}} \langle \mathbf{v} - \mathbf{v}_k, \nabla h_{\mathbf{v}}(\mathbf{U}_{k+1}, \mathbf{v}_k) \rangle + \frac{\lambda}{2} \|\mathbf{v} - \mathbf{v}_k\|^2, \quad (12)$$

where λ, μ are tuning parameters. And as we will see later, as long as they satisfy certain conditions, the updating method above will guarantee the objective is monotonically decreasing.

3.1 Proposed Algorithm

To solve Eq. (11–12), we first derive the solution for \mathbf{U} by fixing \mathbf{V} and dividing into different cases:

3.1.1 Optimizing $\mathbb{U} = \mathbb{U}_1$

To derive the solution we first introduce the following lemma [27]:

Lemma 1. $\max_{\mathbf{X}^T \mathbf{X} = \mathbf{I}} \text{tr}(\mathbf{X}^T \mathbf{B})$ is given by $\mathbf{X} = \mathbf{U} \mathbf{V}^T$, where $[\mathbf{U}, \mathbf{\Sigma}, \mathbf{V}] = \text{svd}(\mathbf{B})$.

Now we can derive the solution to Eq. (11) as follows:

$$\begin{aligned} \mathbf{U}_{k+1} &= \arg \min_{\mathbf{U}^T \mathbf{U} = \mathbf{I}} \langle \mathbf{U} - \mathbf{U}_k, \nabla h(\mathbf{U}_k) \rangle + \frac{\mu}{2} \|\mathbf{U} - \mathbf{U}_k\|_F^2 \\ &= \arg \max_{\mathbf{U}^T \mathbf{U} = \mathbf{I}} \text{tr}(\mathbf{U}^T \mathbf{M}) = \mathbf{Y} \mathbf{Z}^T, \end{aligned} \quad (13)$$

where $\mathbf{M} = 2(\mathbf{X} - \mathbf{U}_k \mathbf{V}_k) \mathbf{V}_k^T + \mu \mathbf{U}_k$ and \mathbf{Y}, \mathbf{Z} is obtained from $[\mathbf{Y}, \mathbf{\Sigma}, \mathbf{Z}] = \text{svd}(\mathbf{M})$.

3.1.2 Optimizing $\mathbb{U} = \mathbb{U}_2$

Similarly, if $\mathbf{U} \geq 0$, then

$$\begin{aligned} \mathbf{U}_{k+1} &= \arg \min_{\mathbf{U} \geq 0} \langle \mathbf{U} - \mathbf{U}_k, \nabla h(\mathbf{U}_k) \rangle + \frac{\mu}{2} \|\mathbf{U} - \mathbf{U}_k\|_F^2 \\ &= \arg \min_{\mathbf{U} \geq 0} \|\mathbf{U} - [\mathbf{U}_k + \frac{2}{\mu} (\mathbf{X} - \mathbf{U}_k \mathbf{V}_k) \mathbf{V}_k^T]\|_F^2 \end{aligned} \quad (14)$$

$$= \max\{\mathbf{U}_k + \frac{2}{\mu} (\mathbf{X} - \mathbf{U}_k \mathbf{V}_k) \mathbf{V}_k^T, 0\}. \quad (15)$$

Now we turn to optimize \mathbf{v}_{k+1} in Eq. (12) given $\|\mathbf{v}\| = l$:

$$\begin{aligned} \mathbf{v}_{k+1} &= \arg \min_{\mathbf{V} \in \mathbb{V}} \langle \mathbf{v} - \mathbf{v}_k, \nabla h(\mathbf{v}_k) \rangle + \frac{\lambda}{2} \|\mathbf{v} - \mathbf{v}_k\|_F^2 \\ &= \arg \max_{\mathbf{V} \in \mathbb{V}} \langle \mathbf{v}, \mathbf{q} \rangle, \end{aligned} \quad (16)$$

where $\mathbf{q} = 2\mathbf{U}_{k+1}^T \mathbf{x} + (\lambda - 2\mathbf{U}_{k+1}^T \mathbf{U}_{k+1}) \mathbf{v}_k$.

In the following various cases, we first set $l = 1$ and then optimize l separately.

3.1.3 Optimizing $\mathbb{V} = \mathbb{V}_1$

We first consider the case that $\mathbb{V} = \mathbb{V}_1$, then apparently $v = \frac{\mathbf{q}}{\|\mathbf{q}\|}$.

3.1.4 Optimizing $\mathbb{V} = \mathbb{V}_2$

In this case, \mathbf{v} is positive and spherically distributed. We can optimize \mathbf{v} by dividing into three cases:

- **Case 1:** When $\mathbf{q} \geq 0$, $J = \|\mathbf{v}\| \|\mathbf{q}\| \cos \theta$, where θ is the angle between \mathbf{v} and \mathbf{q} , obviously $\theta = 0$ will maximize J , thus we have $v^* = \frac{\mathbf{q}}{\|\mathbf{q}\|}$.

- **Case 2:** When \mathbf{q} has mixed signs, we can denote $\mathbf{q} = [\mathbf{q}_+, \mathbf{q}_-]$, where $\mathbf{q}_+ > 0$, while $\mathbf{q}_- \leq 0$. Assume the optimized $\mathbf{v} = [\mathbf{v}_+, \mathbf{v}_-]$ which corresponds to the index of \mathbf{q} with $\mathbf{v}_- \neq 0$ but $\mathbf{v}_+ \geq 0$, then we have:

$$\begin{aligned} \langle \mathbf{v}, \mathbf{q} \rangle &= \langle \mathbf{v}_+, \mathbf{q}_+ \rangle + \langle \mathbf{v}_-, \mathbf{q}_- \rangle \\ &< \langle \mathbf{v}_+, \mathbf{q}_+ \rangle < \left\langle \frac{\mathbf{v}_+}{\|\mathbf{v}_+\|}, \mathbf{q}_+ \right\rangle, \end{aligned} \quad (17)$$

where by following *Case 1*, we have $\mathbf{v}^* = [\frac{\mathbf{q}_+}{\|\mathbf{q}_+\|}; 0; \dots; 0]$.

- **Case 3:** When $\mathbf{q} \leq 0$, the objective \mathbf{J} is equivalent to:

$$\min \mathbf{J} = \langle \mathbf{v}, \bar{\mathbf{q}} \rangle,$$

where $\bar{\mathbf{q}} = -\mathbf{q}$. Since $\mathbf{J} = \|\mathbf{v}\| \|\bar{\mathbf{q}}\| \cos \theta$, which is to maximize the angle between \mathbf{v} and $\bar{\mathbf{q}}$, where both \mathbf{v} and $\bar{\mathbf{q}}$ are nonnegative. Without loss of generality, assume $\bar{\mathbf{q}}$ is in increasing order, then we have:

$$\begin{aligned} \langle \mathbf{v}, \bar{\mathbf{q}} \rangle &= \sum v_i \bar{q}_i \\ &\geq \bar{q}_1 \sum v_i \\ &\geq \bar{q}_1 \end{aligned} \quad (18)$$

where the last line follows from $(\sum v_i)^2 \geq \sum v_i^2 = \|\mathbf{v}\|^2 = 1$ when $\mathbf{v} \geq 0$. The equation holds if and only if $\mathbf{v} = [1; 0 \dots; 0]$.

3.1.5 $\mathbb{V} = \mathbb{V}_3$

WLOG, we assume $\mathbf{q} = [q_1; q_2; \dots; q_r]$ is sorted in an order such that $|q_1| \geq |q_2| \geq \dots \geq |q_r|$, and if we denote $\bar{\mathbf{q}} = [q_1; q_2; \dots; q_s; 0; 0; \dots; 0]$, then $\mathbf{v} = \frac{\bar{\mathbf{q}}}{\|\bar{\mathbf{q}}\|}$.

3.1.6 $\mathbb{V} = \mathbb{V}_4$

Apparently, \mathbb{V}_4 can be regarded as a projection of \mathbb{V}_2 to sparsity constraint. Similarly, it would divide into three cases and only choose the largest s elements in \mathbf{v} before normalization.

Now we turn to optimize l . Taking the derivative w.r.t. l , by setting the gradient to be 0 we obtain:

$$l = \frac{\langle \mathbf{X}, \mathbf{UV} \rangle}{\langle \mathbf{UV}, \mathbf{UV} \rangle}, \quad (19)$$

in any of the cases above. And $\mathbf{V} = l \star \mathbf{V}$ making all the data points reside in the sphere with *radius* = l .

Finally, the algorithm to solve Eq. (5) is summarized in Alg. 1.

4 Convergence Analysis

Before we start the convergence analysis, we first give the lemma below which will be critical to the whole proof [28, 29].

Algorithm 1 Our proposed method to solve Eq. (5)

Input: data $\mathbf{X} \in \mathbb{R}^{m \times n}$, rank of factors r , regularization parameters λ, μ , number of iterations K .

Initialization: $\mathbf{U}^0 \in \mathbb{U}, \mathbf{V}^0 \in \mathbb{V}$,

for $k \leq K$ **do**

optimize \mathbf{U}^{k+1} as Eq. (11) where $\mu \geq 2\sigma_1(\mathbf{V}^k \mathbf{V}^{kT})$,

optimize each \mathbf{v}^{k+1} as Eq. (12) where $\lambda \geq 2\sigma_1(\mathbf{U}^{(k+1)T} \mathbf{U}^{k+1})$,

optimize l as Eq. (19),

end for

Output: \mathbf{U}^K and \mathbf{V}^K .

Lemma 2. For Eq. (9) we have: $\nabla_{\mathbf{U}}^2 h(\mathbf{U}, \mathbf{V}) = 2\mathbf{V}\mathbf{V}^T, \nabla_{\mathbf{V}}^2 h(\mathbf{U}, \mathbf{V}) = 2\mathbf{U}^T \mathbf{U}$, and therefore:

$$h(\mathbf{U}^{k+1}, \mathbf{V}^k) - h(\mathbf{U}^k, \mathbf{V}^k) \leq \langle \mathbf{U}^{k+1} - \mathbf{U}^k, \nabla_{\mathbf{U}} h(\mathbf{U}^k, \mathbf{V}^k) \rangle + \frac{L_{\mathbf{U}}^k}{2} \|\mathbf{U}^{k+1} - \mathbf{U}^k\|_F^2, \quad (20)$$

$$h(\mathbf{U}^{k+1}, \mathbf{V}^{k+1}) - h(\mathbf{U}^{k+1}, \mathbf{V}^k) \leq \langle \mathbf{V}^{k+1} - \mathbf{V}^k, \nabla_{\mathbf{V}} h(\mathbf{U}^{k+1}, \mathbf{V}^k) \rangle + \frac{L_{\mathbf{V}}^k}{2} \|\mathbf{V}^{k+1} - \mathbf{V}^k\|_F^2,$$

where $L_{\mathbf{U}}^k = \sigma_1(\nabla_{\mathbf{U}}^2 h(\mathbf{U}, \mathbf{V})) = 2\sigma_1(\mathbf{V}^k \mathbf{V}^{kT}), L_{\mathbf{V}}^k = \sigma_1(\nabla_{\mathbf{V}}^2 h(\mathbf{U}, \mathbf{V})) = 2\sigma_1(\mathbf{U}^{(k+1)T} \mathbf{U}^{k+1})$ and $\sigma_1(\mathbf{X})$ denotes the largest eigenvalue of \mathbf{X} .

To analyse the convergence, we rewrite Eq. (9) as

$$\min_{\mathbf{U}, \mathbf{V}} f(\mathbf{U}, \mathbf{V}) = h(\mathbf{U}, \mathbf{V}) + \delta_{\mathbb{U}}(\mathbf{U}) + \delta_{\mathbb{V}}(\mathbf{V}), \quad (21)$$

where $\delta_{\mathbb{U}}(\mathbf{U}) = \begin{cases} 0, & \mathbf{U} \in \mathbb{U} \\ \infty, & \mathbf{U} \notin \mathbb{U} \end{cases}$ is the indicator function of the set \mathbb{U} and therefore nonsmooth, so is $\delta_{\mathbb{V}}(\mathbf{V})$.

The following result establishes that the subsequence convergence property of the proposed algorithm.

Theorem 1. Let $\{\mathbf{W}_k\}_{k \geq 0} = \{(\mathbf{U}_k, \mathbf{V}_k)\}_{k \geq 0}$ be the sequence generated by Algorithm 1 with regularization parameter $\lambda^k \geq \bar{L}_{\mathbf{V}}^{k-1}, \mu^k \geq L_{\mathbf{U}}^{k-1}$, then the objective in Eq. (9) is monotonically non-increasing.

Proof. First note that for all k , according to Algorithm 1, we always have $\delta_{\mathbb{U}}(\mathbf{U}_k) = \delta_{\mathbb{V}}(\mathbf{V}_k) = 0$ and accordingly $f(\mathbf{U}^k, \mathbf{V}^k) = h(\mathbf{U}^k, \mathbf{V}^k)$. By the definition of Lipschitz continuous gradient and Taylor expansion, we have

$$h(\mathbf{U}^k, \mathbf{V}^{k-1}) - h(\mathbf{U}^{k-1}, \mathbf{V}^{k-1}) \leq \langle \mathbf{U}^k - \mathbf{U}^{k-1}, \nabla_{\mathbf{U}} h(\mathbf{U}^{k-1}, \mathbf{V}^{k-1}) \rangle + \frac{L_{\mathbf{U}}^{k-1}}{2} \|\mathbf{U}^k - \mathbf{U}^{k-1}\|_F^2. \quad (22)$$

Also by the definition of proximal map, we get:

$$\mathbf{U}_k = \arg \min_{\mathbf{U}} \delta_{\mathbb{U}}(\mathbf{U}) + \frac{\mu^k}{2} \|\mathbf{U} - \mathbf{U}_{k-1}\|_F^2 + \langle \nabla_{\mathbf{U}} h(\mathbf{U}_{k-1}, \mathbf{V}_{k-1}), \mathbf{U} - \mathbf{U}_{k-1} \rangle. \quad (23)$$

Therefore, we have $f(\mathbf{U}_k, \mathbf{V}_{k-1}) \leq f(\mathbf{U}_{k-1}, \mathbf{V}_{k-1})$, which implies the following:

$$\delta_{\mathbb{U}}(\mathbf{U}_k) + \frac{\mu^k}{2} \|\mathbf{U}_k - \mathbf{U}_{k-1}\|_F^2 + \langle \nabla_{\mathbf{U}} h(\mathbf{U}_{k-1}, \mathbf{V}_{k-1}), \mathbf{U}_k - \mathbf{U}_{k-1} \rangle \leq \delta_{\mathbb{U}}(\mathbf{U}_{k-1}). \quad (24)$$

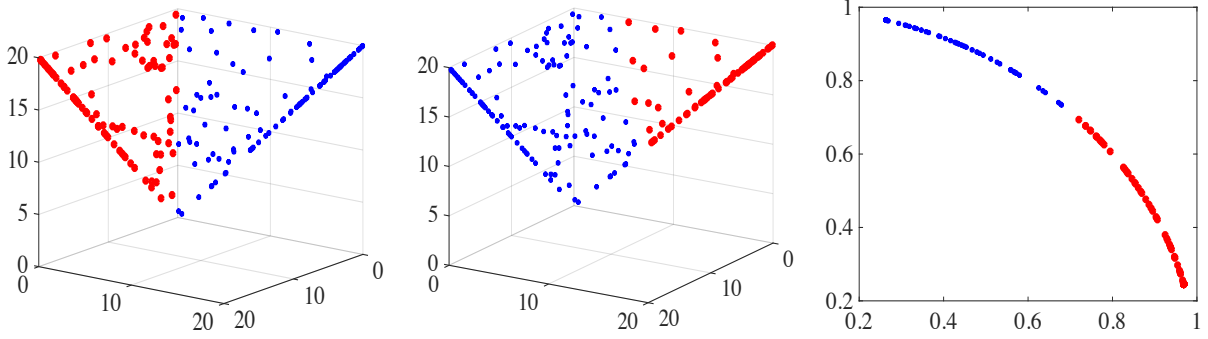


Figure 3: **Left:** two groups of data generated from two angles. **Center:** clustering result with distance-based method K -means. **Right:** projection into \mathbf{V} via factorization $\mathbf{X} \approx \mathbf{UV}$ where $\mathbf{U} \in \mathbb{U}_1, \mathbf{V} \in \mathbb{V}_2$. Blue and red represent different clusters [1].

Combining Eq. (22) to Eq. (24), we have:

$$\begin{aligned}
& h(\mathbf{U}_k, \mathbf{V}_{k-1}) + \delta_{\mathbb{U}}(\mathbf{U}_k) \\
& \leq h(\mathbf{U}_{k-1}, \mathbf{V}_{k-1}) + \langle \nabla_{\mathbf{U}} h(\mathbf{U}_{k-1}, \mathbf{V}_{k-1}), \mathbf{U}_k - \mathbf{U}_{k-1} \rangle + \frac{L_U^{k-1}}{2} \|\mathbf{U}_k - \mathbf{U}_{k-1}\|_F^2 + \delta_{\mathbb{U}}(\mathbf{U}_k) \\
& \leq h(\mathbf{U}_{k-1}, \mathbf{V}_{k-1}) + \frac{L_U^{k-1}}{2} \|\mathbf{U}_k - \mathbf{U}_{k-1}\|_F^2 + \delta_{\mathbb{U}}(\mathbf{U}_{k-1}) - \frac{\mu^k}{2} \|\mathbf{U}_k - \mathbf{U}_{k-1}\|_F^2 \\
& = h(\mathbf{U}_{k-1}, \mathbf{V}_{k-1}) + \delta_{\mathbb{U}}(\mathbf{U}_{k-1}) - \frac{\mu^k - L_U^{k-1}}{2} \|\mathbf{U}_k - \mathbf{U}_{k-1}\|_F^2.
\end{aligned} \tag{25}$$

Similarly, we have

$$h(\mathbf{U}_k, \mathbf{V}_k) - h(\mathbf{U}_k, \mathbf{V}_{k-1}) + \delta_{\mathbb{V}}(\mathbf{V}_k) - \delta_{\mathbb{V}}(\mathbf{V}_{k-1}) \leq -\frac{\lambda^k - L_V^{k-1}}{2} \|\mathbf{V}_k - \mathbf{V}_{k-1}\|_F^2, \tag{26}$$

which illustrates within each update, the objective is non-increasing if $\lambda^k > L_V^{k-1}, \mu^k > L_U^{k-1}$. \square

Global sequence convergence property and at least sub-linear convergence rate can be proved by following [26, 30].

5 Experiment

We will carefully examine the effectiveness of our proposed method including spherical nonnegative matrix factorization (on synthetic data) and PCA (real-world data) respectively.

5.1 Synthetic Data

We first generate 200 data points, half of which is distributed within the region between $\mathbf{X} = \mathbf{Z}$ and \mathbf{Z} axis (denoted as blue dots in the left part of Fig. 3, while another group is generated within the region between $\mathbf{Y} = \mathbf{Z}$ and \mathbf{Z} axis (denoted as the red dots). These two clusters of data are generated through different angles. Thus when we do clustering, it should be angle distance rather than Euclidean distance to determine

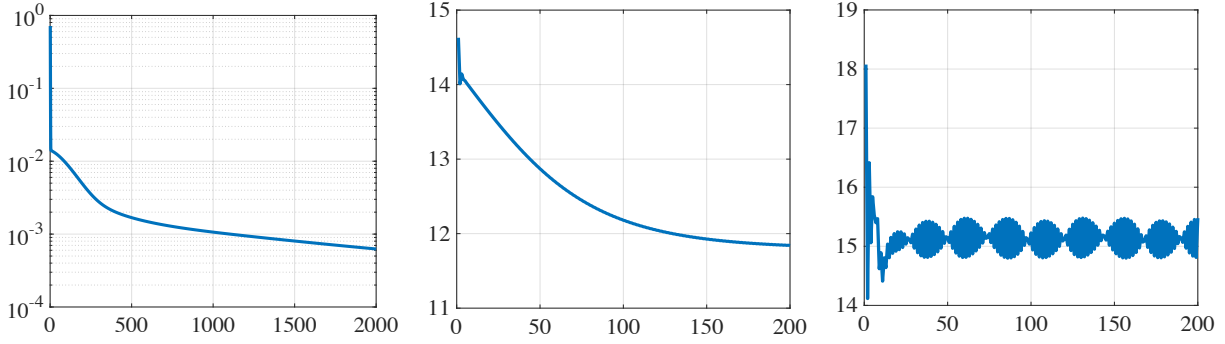


Figure 4: **Left:** Typical $\|U_{k+1} - U_k\|_F$ with updates. **Center:** Objective converges when λ is sufficiently large. **Right:** Objective oscillates when λ is relatively small.

the clustering result. For our method, we learn a feature matrix $U \in \mathbb{R}^{3 \times 2}$ and plot the component matrix $V \in \mathbb{R}^{2 \times 200}$ as the Right part illustrates. We see that, Euclidean distance-based method (such as K -means) will yield poor clustering result (middle part), while ours will obtain good clustering result (due to the data’s generation method, they can be separated by anti-diagonal).

Also, we show the convergence of $\{W_k\}_{k \geq 0} = \{(U_k, V_k)\}_{k \geq 0}$ generated by our method. As Fig. 4 shows, after short iterations, the generated sequences will be stable, which is in accordance with the convergence proof. Fig. 4 also illustrates that the objective with update. We also see that only sufficiently large λ , μ will make objective monotonically decreasing.

5.2 Real-world Datasets Experiment

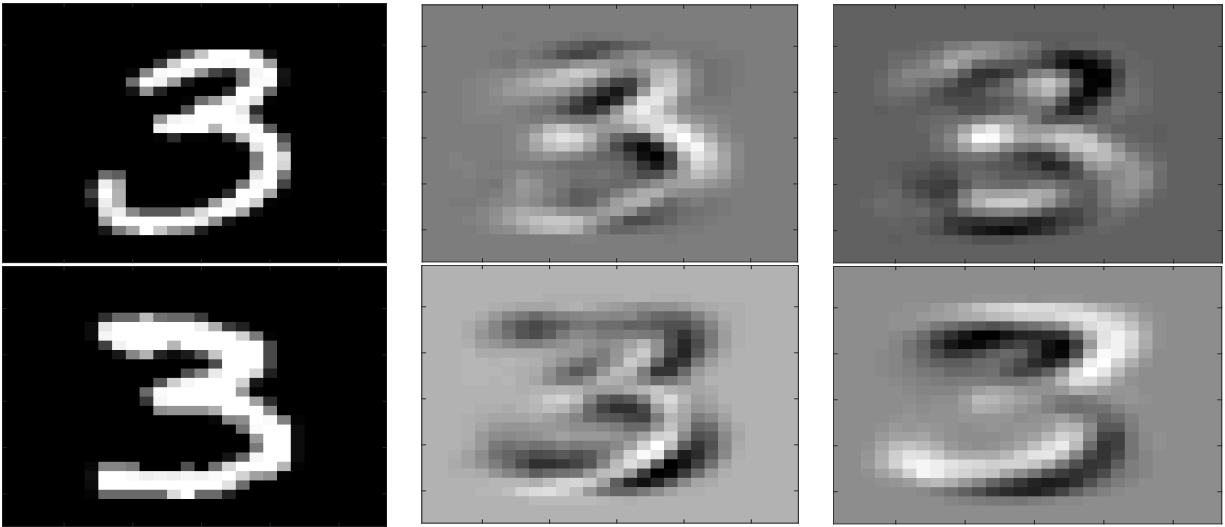


Figure 5: **Left:** original images x ; **Center:** u corresponds to the largest coefficient; **Right:** u corresponds to second largest coefficient. In this setting, $U \in \mathbb{U}_1, V \in \mathbb{V}_4$.

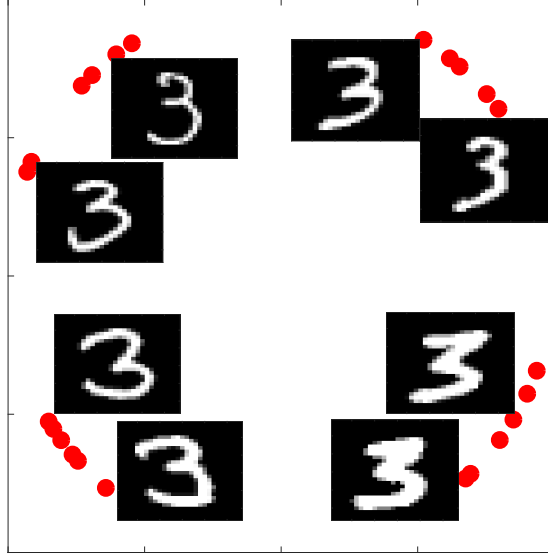


Figure 6: All data point is distributed in the sphere, we see the images with similar pattern lie close to each other. From left to right, the tail becomes shorter while from bottom to top the size turns smaller.

In this subsection, we will first test our proposed method on *MNIST handwritten digits* dataset [31]. We collect all images of digit three from the test set image file which give 1010 images. The original image is 28×28 , which corresponds to $m = 784$ dimension feature. We set $r = 10$, that is to project into 10 dimensional space, then U is made up with 10 mutually orthogonal vectors. Each image data in the new coordinate system is represented as v . To demonstrate the effectiveness in light of visualization, we set $s = 2$, that is every original data is approximated by the linear combination of top 2 features in u . Fig. 5 illustrates the most critical features. We see the first learned component has very similar pattern as original image. We plot these data where u_1 and u_2 are the principal component vectors as Fig. 6 demonstrates, where X -axis and Y -axis corresponds to the first and second element in v . The first and second row image in Fig. 5 lie in the second and third quadrant in Fig. 6, where they share the similar first component but varies in second component. We see that our proposed method can yield reasonable and promising results even we project from original high dimension space into very low one.

References

- [1] K. Liu, Q. Li, H. Wang, and G. Tang, "Spherical principal component analysis," in *Proceedings of the 2019 SIAM International Conference on Data Mining*, pp. 387–395, SIAM, 2019.
- [2] D. D. Lee and H. S. Seung, "Learning the parts of objects by non-negative matrix factorization," *Nature*, vol. 401, no. 6755, p. 788, 1999.
- [3] K. Liu, *A Study of Non-Negative Matrix Factorizations: Foundations, Methods, Algorithms, and Applications*. Colorado School of Mines, 2019.

- [4] W. Xu, X. Liu, and Y. Gong, “Document clustering based on non-negative matrix factorization,” in *Proceedings of the 26th annual international ACM SIGIR conference on Research and development in informaion retrieval*, pp. 267–273, ACM, 2003.
- [5] K. Liu and H. Wang, “Robust multi-relational clustering via ℓ_1 -norm symmetric nonnegative matrix factorization-norm symmetric nonnegative matrix factorization,” in *Proceedings of the 53rd Annual Meeting of the Association for Computational Linguistics and the 7th International Joint Conference on Natural Language Processing (Volume 2: Short Papers)*, pp. 397–401, 2015.
- [6] K. Liu and H. Wang, “High-order co-clustering via strictly orthogonal and symmetric ℓ_1 -norm nonnegative matrix tri-factorization,” in *Proceedings of the Twenty-Seventh International Joint Conference on Artificial Intelligence*, 2018.
- [7] M. N. Schmidt and R. K. Olsson, “Single-channel speech separation using sparse non-negative matrix factorization,” in *Ninth International Conference on Spoken Language Processing*, 2006.
- [8] P. Smaragdis and J. C. Brown, “Non-negative matrix factorization for polyphonic music transcription,” in *Applications of Signal Processing to Audio and Acoustics, 2003 IEEE Workshop on.*, pp. 177–180, IEEE, 2003.
- [9] J. S. Lee, D. D. Lee, S. Choi, and D. S. Lee, “Application of nonnegative matrix factorization to dynamic positron emission tomography,” in *3rd International Conference on Independent Component Analysis and Blind Signal Separation*, pp. 556–562, 2001.
- [10] P. M. Rossini, A. Barker, A. Berardelli, M. Caramia, G. Caruso, R. Cracco, M. Dimitrijević, M. Hallett, Y. Katayama, C. Lücking, *et al.*, “Non-invasive electrical and magnetic stimulation of the brain, spinal cord and roots: basic principles and procedures for routine clinical application. report of an ifcn committee,” *Electroencephalography and clinical neurophysiology*, vol. 91, no. 2, pp. 79–92, 1994.
- [11] V. K. Potluru and V. D. Calhoun, “Group learning using contrast nmf: Application to functional and structural mri of schizophrenia,” in *2008 IEEE International Symposium on Circuits and Systems*, pp. 1336–1339, IEEE, 2008.
- [12] K. Liu, H. Wang, S. Risacher, A. Saykin, and L. Shen, “Multiple incomplete views clustering via non-negative matrix factorization with its application in alzheimer’s disease analysis,” in *2018 IEEE 15th International Symposium on Biomedical Imaging (ISBI 2018)*, pp. 1402–1405, IEEE, 2018.
- [13] F. Yu, Q. Liu, S. Wu, L. Wang, and T. Tan, “A dynamic recurrent model for next basket recommendation,” in *Proceedings of the 39th International ACM SIGIR conference on Research and Development in Information Retrieval*, pp. 729–732, ACM, 2016.
- [14] M. R. Blanton and S. Roweis, “K-corrections and filter transformations in the ultraviolet, optical, and near-infrared,” *The Astronomical Journal*, vol. 133, no. 2, p. 734, 2007.
- [15] O. Berne, C. Joblin, Y. Deville, J. Smith, M. Rapacioli, J. Bernard, J. Thomas, W. Reach, and A. Abergel, “Analysis of the emission of very small dust particles from spitzer spectro-imagery data using blind signal separation methods,” *Astronomy & Astrophysics*, vol. 469, no. 2, pp. 575–586, 2007.
- [16] D. D. Lee and H. S. Seung, “Algorithms for non-negative matrix factorization,” in *Advances in neural information processing systems*, pp. 556–562, 2001.

- [17] C. H. Ding, T. Li, and M. I. Jordan, “Convex and semi-nonnegative matrix factorizations,” *IEEE transactions on pattern analysis and machine intelligence*, vol. 32, no. 1, pp. 45–55, 2010.
- [18] C. Ding, T. Li, W. Peng, and H. Park, “Orthogonal nonnegative matrix t-factorizations for clustering,” in *Proceedings of the 12th ACM SIGKDD international conference on Knowledge discovery and data mining*, pp. 126–135, ACM, 2006.
- [19] V. Tunali, T. Bilgin, and A. Camurcu, “An improved clustering algorithm for text mining: Multi-cluster spherical k-means,” *International Arab Journal of Information Technology (IAJIT)*, vol. 13, no. 1, 2016.
- [20] A. Singhal *et al.*, “Modern information retrieval: A brief overview,” *IEEE Data Eng. Bull.*, vol. 24, no. 4, pp. 35–43, 2001.
- [21] I. S. Dhillon and D. S. Modha, “Concept decompositions for large sparse text data using clustering,” *Machine learning*, vol. 42, no. 1, pp. 143–175, 2001.
- [22] H. Hou, “A fast recursive algorithm for computing the discrete cosine transform,” *IEEE Transactions on Acoustics, Speech, and Signal Processing*, vol. 35, no. 10, pp. 1455–1461, 1987.
- [23] H. V. Nguyen and L. Bai, “Cosine similarity metric learning for face verification,” in *Asian conference on computer vision*, pp. 709–720, Springer, 2010.
- [24] P. L. Combettes and T. Pennanen, “Proximal methods for cohyppomonotone operators,” *SIAM journal on control and optimization*, vol. 43, no. 2, pp. 731–742, 2004.
- [25] A. Kaplan and R. Tichatschke, “Proximal point methods and nonconvex optimization,” *Journal of global Optimization*, vol. 13, no. 4, pp. 389–406, 1998.
- [26] J. Bolte, S. Sabach, and M. Teboulle, “Proximal alternating linearized minimization or nonconvex and nonsmooth problems,” *Mathematical Programming*, vol. 146, no. 1-2, pp. 459–494, 2014.
- [27] N. Higham and P. Papadimitriou, “Matrix procrustes problems,” *Rapport technique, University of Manchester*, 1995.
- [28] X. Zhou, “On the fenchel duality between strong convexity and lipschitz continuous gradient,” *arXiv preprint arXiv:1803.06573*, 2018.
- [29] K. Liu, X. Li, Z. Zhu, L. Brand, and H. Wang, “Factor-bounded nonnegative matrix factorization,” *ACM Transactions on Knowledge Discovery from Data (TKDD)*, vol. 15, no. 6, pp. 1–18, 2021.
- [30] Z. Zhu, X. Li, K. Liu, and Q. Li, “Dropping symmetry for fast symmetric nonnegative matrix factorization,” *arXiv preprint arXiv:1811.05642*, 2018.
- [31] Y. LeCun, L. Bottou, Y. Bengio, and P. Haffner, “Gradient-based learning applied to document recognition,” *Proceedings of the IEEE*, vol. 86, no. 11, pp. 2278–2324, 1998.